Global NEST Journal, Vol 23, No 1, pp 137-142

Influence of calcination conditions on the adsorption properties of the wasted sea shell to the dibutyl phthalate

Zhao L.[1], Fang Y.[1], Xu X.[2], Xu J.[1] and Qin S.[1]*
[1]Department of Environment Science & Safety Engineering, Tianjin University of Technology, Tianjin, 300384, China
[2]Tianjin Bohai Vocational Technical College, Tianjin 300402, China
Received: 16/07/2019, Accepted: 11/04/2021, Available online: 20/05/2021
*to whom all correspondence should be addressed: e-mail: qinsongyan@vip.126.com
https://doi.org/10.30955/gnj.003187

Graphical abstract

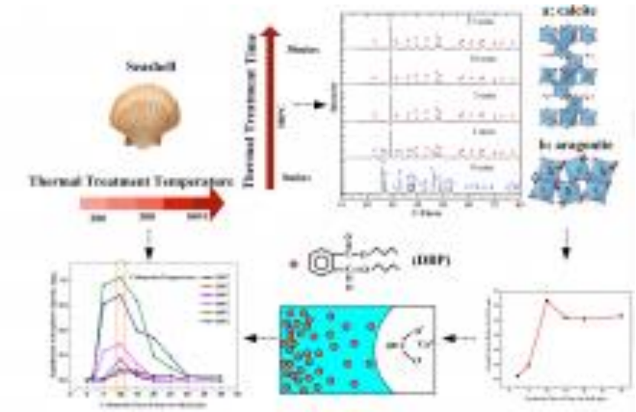

Abstract

The calcined clam seashell powders were applied as adsorbent to adsorb Dibutyl phthalate (DBP), from an aqueous solution. The influence of calcination conditions including temperature and time on its adsorption capability to DBP was investigated. The shell powders calcined at 500 °C had the best adsorption capability. As the calcination time extending under different temperatures, the adsorption capabilities showed the same tendency and reached peak values at the calcination time of 10mins. Calcination time extension also led to the increase of crystal unit cell Sizes of $CaCO_3$ inside the clam seashells at the first 10mins and then decreased to the stable value. Correspondingly, the calcined shell specific surface areas decreased firstly to the minimum at 10mins and then gradually increased, as the calcination process lasting at 500°C. The maximum adsorption capability as 1.237mg/g, the lowest specific surface area as 14.2m^2/g, and the largest unit cell size as 60.7nm of $CaCO_3$ simultaneously exhibited at the calcination time of 10mins. The Freundlich isotherm model and the pseudo-second-order-kinetics model were appropriate for describing the adsorption isotherm and kinetics of DBP at 30°C, respectively. It is inferred that the interaction between calcined shell and DBP is chemical adsorption.

Key Words: adsorption, calcination, clam sea shell, dibutyl Phthalate (DBP), thermal treatment.

1. Introduction

Dibutyl phthalate (DBP) has been extensively concerned because of its widespread existence as an endocrine-disrupting compound (EDC), which leads to the reduction of reproductive ability or the other reproductive disorders via interaction with the endocrine system (Wang *et al.*, 2016).DBP has been included as a priority pollutant of the US-EPA (EPA, 2014), the European Union (EU) (CSWDICSED, 2007) and the Chinese water list (NSPRC, 2006). It has been detected in worldwide sea and surface water bodies. DBP was widely detected in 21 out of 23 sampling sites in the urban lakes in Guangzhou, China, its concentration was high as 1840 ng/L (Zhang *et al.*, 2019). In Bohai bay between China and Korea, DBP was reported to vary from 266-1584ng/L mainly caused by the industrial wastewater discharge (Li *et al.*, 2017). Due to its accumulation in the fishery product which then poses a potential health threat to humans through the food chain, DBP removal from the waterbody is urgent.

The prevailing DBP removal techniques focus on catalytic degradation such as photocatalytic ozonation over TiO_2 film (Li *et al.*, 2005), nano photocatalytic Fe, Ag-ZnO/VIS-LED system (Akbari-Adergani *et al.*, 2018), or by copper-based metal-organic frameworks coupled with persulfate (Li *et al.*, 2018). Although they are efficient, these methods still need to solve the problems such as heterogeneous chemicals introduced to the waterbody when applied to the in-situ remediation. Adsorption is an effective way for waterbody in-situ remediation (Suresh *et al.*, 2012). The adsorption of DBP from aqueous solution using phoenix leaves activated carbon (PLAC) by chemical activation with phosphate was investigated. Synthetic adsorbents such as resin have also been studied to establish their removal efficiency toward PAEs (Zhang *et al.*, 2008). Researchers have also developed an intense interest in the modification of adsorbent surfaces to enhance their adsorptive efficiency as well as their stability that provides essential functionalization to trap the target analyte (Qureshi *et al.*, 2012). However, those methods and techniques still pose a

Zhao L., Fang Y., Xu X., Xu J. and Qin S. (2021), Influence of calcination conditions on the adsorption properties of the wasted sea shell to the dibutyl phthalate, *Global NEST Journal*, **23**(1), 137-142.

potential risk to introduce heterogeneous chemicals into the waterbody. The low-cost and environmentally friendly adsorbent should be developed, as the large volume of water resources was economically purified (Doke *et al.*, 2013).

The waste seashell is an abundant and cheap renewable resource. Its resourceful utility technique is urgently needed to develop to release the landfill burden and reduce the disposal cost (Ning and Xi, 2015). Its microstructure is the $CaCO_3$ crystal group enchased by the 3-D net organic chitin. The porous $CaCO_3$ materials can be obtained by the calcination of seashells. Therefore, it should be a feasible sorbent of calcic-series (Bi, 2002; Lin, 2010). The excellent adsorption abilities of different calcined seashells had already been proved. Xiong (2011) have calcined mussel shell powder at 700℃ for 20 min to adsorb the phosphate from an aqueous solution. The phosphate removal capacity is enhanced, from 25% to 55%, when the pH is 5.5. The adsorption isotherm tests showed the Temkin and D-R equations are suitable for the adsorption. Chowdhury (2010) have dried bivalve-type seashells at 383 ± 1 K for 24 h, then investigated the prepared shell adsorption ability to the cationic dye-Basic Green 4 (BG 4) from aqueous solution. It is revealed that–OH, $–CO_3$, and$–PO_4$ functional groups were mainly responsible for the adsorption process. Pena (Peña-Rodríguez *et al.*, 2013) determined mercury retention on the calcined and ground mussel shells, she proved the higher Hg adsorption on the calcined shell would be related to its calcite and dolomite concentrations. Past studies mainly focus on the polar and cationic adsorbates adsorption by the calcined shell, seldom are related to unipolar adsorbates, especially for DBP, it's more difficult to be adsorbed due to its aromatic ring and long-chain carboxy structure. Besides, as seashell calcining, its characteristics, such as crystal structure, special surface area, *etc.*, would be modified, its adsorption ability would be correspondingly changed. However, The effect of the calcination process on the adsorption ability is seldom studied. The objective of this study was to investigate how the structure evolvement of sea shell during the adsorption process influence the DBP adsorption capacity. Adsorption kinetics and isotherms were also evaluated. This paper provides a new idea to develop waste seashells as environmentally friendly adsorbents for DBP removal.

2. Materials and methods

2.1. Adsorbent preparation

The waste clam seashells used in experiments were collected from Bohai Bay in Tianjin, China. The seashells were washed with water and dried at 105 °C. Then they were mashed in an iron mortar into the powders with particle size less than 50 mesh. The Thermal Gravity Analysis (TGA, TG AQ50, Waters) of the powders was carried out firstly, to get the decomposition temperatures of different components. 1g of the seashell powder was calcined in the muffle furnace under the air atmosphere. Various temperature and time as parameters were applied in the calcination process. The specific surface area (V-Sorb 2800S BET surface area analyzer, Gold APP Instruments), XRD (D/Max 2500, RIGAKU) of calcined powder was analyzed. Crystal size was calculated by MDI Jade 5.0 software according to the data of their XRD spectra. Then its adsorption capability of DBP was investigated.

2.2. Adsorption experiment

0.2g of the calcined powder was added into 100ml of DBP solution. The suspension was stirred at 200rpm under 30°C for the specified time. Then the powders were separated by filtration, and the residual DBP of filter liquor was determined by UV spectrophotometry. The adsorption capacity was calculated by Eq. (1):

$$q_t = \frac{(C_0 - C_t)V}{m} \tag{1}$$

Where q_t (mg·g^{-1}) is the DBP adsorption capacity of calcined powder after adsorption for *t* (mins) time, C_0 (mg·L^{-1}) is the initial DBP concentration in solution, C_t (mg·L^{-1}) is the DBP concentration in solution at *t* time, *V* (mL) is the volume of the solution, and *m* (g) is the mass of the calcined powder. At the adsorption equilibrium, q_t is replaced by the equilibrium adsorption capacity, q_e in Eq. (1), and C_t is replaced by the DBP equilibrium concen-tration in solution, C_e. All adsorption experiments were performed in triplicate, and the mean values were used in data analysis.

The DBP adsorption kinetics was carried out in a batch system. 0.2g of sample (calcined at 500°C for 10mins) was mixed in 100mL DBP solution (10mg/L). The adsorption process lasted for the predetermined time at 30°C under agitation. The series of predetermined time was from 1 to 60mins. Two kinetics models, the pseudo-first-order kinetic model, and the pseudo-second-order kinetic model were fitted to experimental data using the linear regression method (Origin 8.1) (Qiu *et al.*, 2009).

The DBP adsorption equilibrium studies were also carried out in a batch system. 0.2g of sample (calcined at 500°C for 10mins) was mixed in 100mL DBP solution, and the initial DBP concentrations of the solutions were 2, 5, 10, 20, 30 and 40 mg/L. The adsorption process lasted for more than 60 mins at 30°C under agitation, to achieve adsorption equilibrium. Two adsorption isotherms models, Langmuir and Freundlich equilibrium models, were fitted to experimental data.

3. Results and discussions

3.1. The thermal gravity analysis

Figure 1 is the TGA of clam sea shell powder under the air atmosphere. The thermogravimetric curve showed that its thermal decomposition included four stages. The first stage was water loss from room temperature to 120.04°C, and the weight loss rate was 0.4675%. The second stage was the partial decomposition of organic chitin from 120.04°C to 240.07 °C, and the loss rate was 1.214%. The third stage was the decomposition of the residual organic chitin from 240.07°C to 359.29°C, and the loss rate was 1.206%. The last stage was the decomposition of $CaCO_3$ from 535.28 °C to 738.84°C, and the loss rate was 41.72%.

The final residue should be CaO, and its mass fraction was 54.81%. According to the residual rate and excluding water, the mass fraction of $CaCO_3$ among clam seashell should be 94.82%, then that of the organic chitin should be 5.18%.

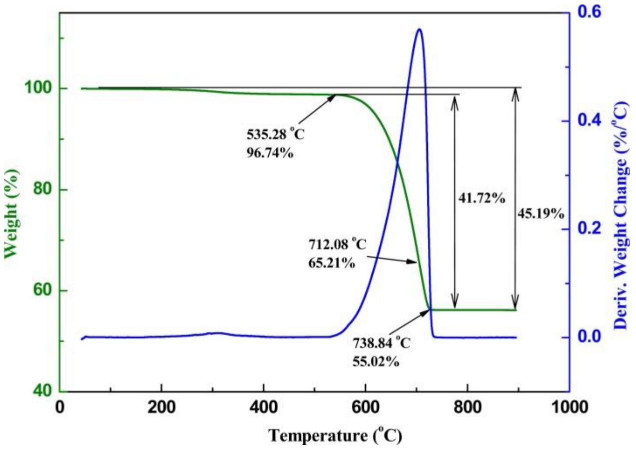

Figure 1. TGA of clam sea shell powder under air atmosphere

The TGA also turned out that the initial decomposition temperature of $CaCO_3$ of clam sea shell was 535.28 °C. Therefore the calcination temperature of shell powers was limited low than 550 °C, or else $CaCO_3$ would turn into water-soluble CaO.

3.2. The influences of Calcination conditions on adsorption capability

Figure 2 was the calcination residual rate of the clam sea shell under different conditions. It turned out that the residual rates decreased with the rise of the calcination temperature, which was consistent with the TGA of clam seashells. At 500 °C, the calcination time of 2 mins was long enough for the decomposition of organic matter, while at other calcination temperatures, the residual rate slightly decreased with the increase of calcination time. The residual rates at 550°C were lower than 92%, which means most of $CaCO_3$ converted into CaO.

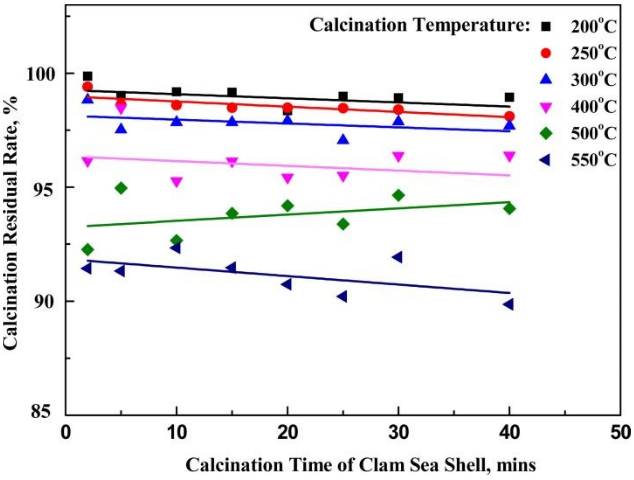

Figure 2. The calcination residual rate of clam sea shell under different conditions

Figure 3 showed the equilibrium adsorption capability of shell powder prepared under different calcination conditions.

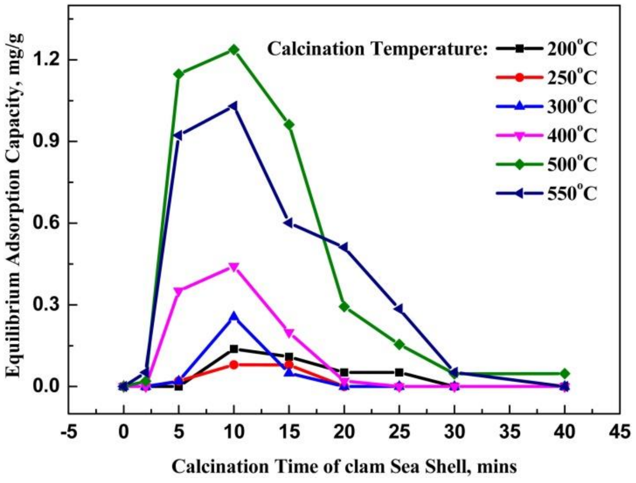

Figure 3. The equilibrium adsorption capability of shell powder prepared under different calcination conditions

It illustrated that the calcination conditions significantly affected the adsorption capabilities of the adsorbent. Calcination temperature exerts a positive effect on the adsorption capabilities when the temperature is no more than 500 °C. However, when the temperature increased to 550 °C, the adsorption capability decreased moderately. The shell calcinated at 500 °C has a better adsorption capability than samples at other temperatures. It is also noticeable that the adsorption capability increased four times when the calcination temperature raised from 400 °C to 500 °C. One reason could be the existence of organic matter weighted against the adsorption of DBP. As the calcination temperature increasing, the residue of organic matter decreased, therefore the adsorption capability was improved accordingly. As for the decaying adsorption capability of shell calcined at 550°C, the decomposition of part of $CaCO_3$ was the main reason.

Figure 3 also showed that the calcination time affected the adsorption behavior of the shell to a great extend. As time extending under any calcination temperatures, the adsorption capabilities of shell powder had the same changing trend: fleetly increasing firstly until all shell samples reached their maximum adsorption capability at the calcination time of 10mins, then decreased. all organic matter burned out among 2mins at 500°C, and the residual rate of sea shell kept unchanged as time going. Therefore, almost all the residue should be $CaCO_3$, which can not be decomposed at this temperature. But the adsorption capability still fluctuated acutely as the calcination time going. This phenomenon implied that some characteristics of seashell which could remarkably impact its adsorption capability were changing as the calcination time increasing.

3.3. Microstructure evolvement during the calcination process

Figure 4 was the XRD spectra of the clam seashell calcined at 500°C for different times. These spectra turned out that the crystal form of $CaCO_3$ inside the clam seashell converted from the aragonite to the calcite during the calcination at 500°C. The calcination time of 5mins was long enough for the change of the crystal form. There was no obvious difference seemingly among the XRD shapes of the calcite crystal as the calculations process going, but the size of these crystal cells changed with some rules.

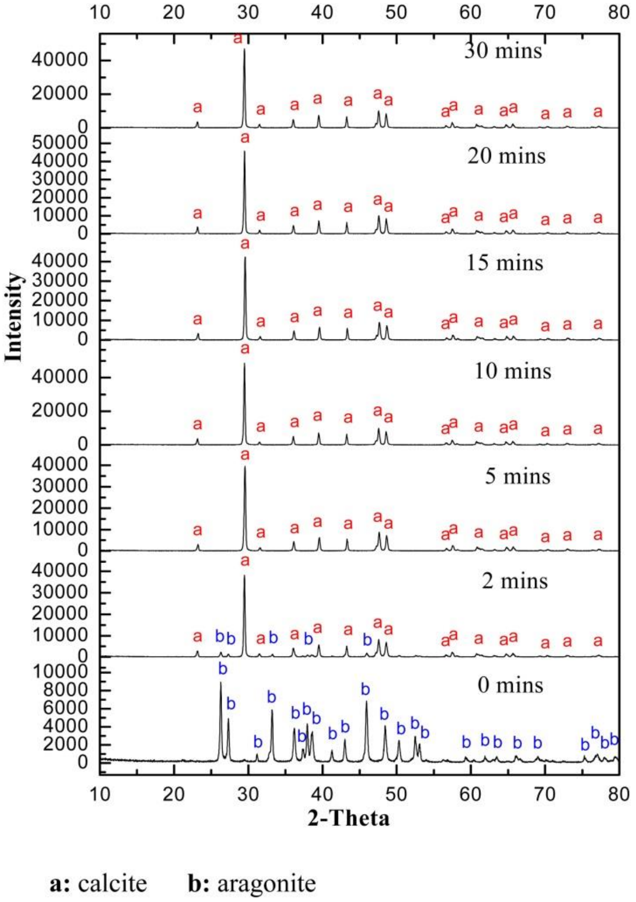

Figure 4. The XRD spectra of the clam sea shell calcined at 500°C for different time

Figure 5 was the crystal unit cell sizes of $CaCO_3$ inside the clam seashells calcined at 500°C for different times. During the clam seashells calcining, the crystal form of $CaCO_3$ changed from the aragonite to the calcite. At the calcination time of 2mins, the majority had converted, which could be proved by Figure 4. The unit cell size of the initial calcite was only 50.5nm, the cell shape was not perfect. As the calcination process going, the thermal treatment made the calcite crystal gradually perfect. The unit cell rapidly swelled to the largest size, 60.7nm at 10min, and then slightly shrank to the stable size, around 58nm.

The adsorption capabilities change associated extremely with the change of crystal cell size and show a positive relationship. (Figure 1) The larger the unit cell size was, the better the adsorption capability toward DBP exhibited. The best adsorption capability and the largest unit cell size simultaneously occurred at the calcination time of 10mins.

The specific surface areas of the clam seashells calcined at 500°C for different calcination times were correspondingly analyzed, as shown in Figure 6. It is unexpected that the change tendency of specific surface areas related negatively with the crystal cell size, surface area decreased firstly and reached to the smallest as the crystal cell increased to the biggest size at the calcination time of 10mins, and then gradually increased as the calcination lasting.

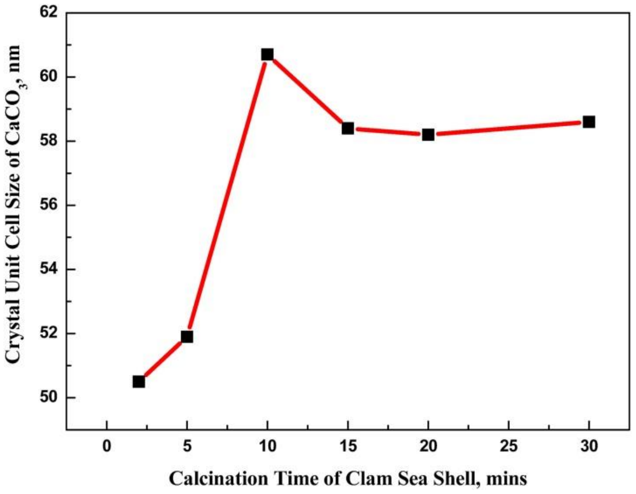

Figure 5. The crystal unit cell Sizes of $CaCO_3$ inside the clam seashells calcined at 500°C for different time

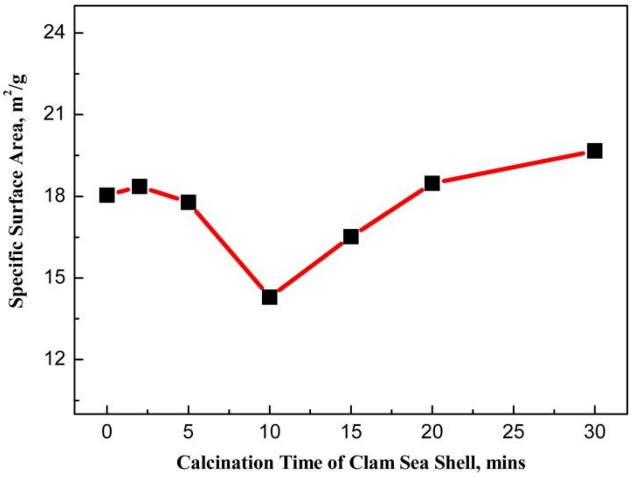

Figure 6. The specific surface areas of clam seashells calcined at 500°C for different time

Specific surface area is an important parameter influencing on adsorption capability of adsorbents. It was well known that the adsorption capability of adsorbents should be improved as its specific surface area increased. But in this paper, the relationship between them was different from the common concept. The adsorption capability reached the maximum when the surface area became the smallest, and then adsorption capability decreased as its specific surface area increases. This phenomenon implied that the specific surface area was not the determinant factor of the adsorption capability, compared with other factors such as adsorbent and adsorbate structure. Adsorb and/or promote polymerization of organic molecules on the mineral surface is an important process for the interaction between mineral and organic molecules. It is widely recognized that adsorption/desorption rate-limiting steps can be related to the size, structural defects, and morphology of the nanostructures. Previous studies also showed that adsorption of organic molecules is favored when at least two carboxylate groups are involved in bidentate coordination to surface atoms. Carbonyl groups often play a significant role in linkage and surface adsorption processes (Teng and Dove, 1997). Lee and Reeder (Lee and Reeder, 2006) proved that the adsorption mechanisms related to the interaction between minerals and large organic molecules such as bis-(2-ethylhexyl) phthalate (DEHP) can occur via physical and/or chemical reactions involving different surface sites. An example of organic molecules absorption onto nanocrystalline minerals, the Binding of DEHP at the surface of hydrozincite nanocrystals, shows the chemical interactions involving C=O groups of DEHP and atomic sites at the hydrozincite nanocrystals surface. It is characterized as the Oxygen atom binding of the C=O group of DEHP and the Zn-O at the surface polyhedral. So it may be inferred that a similar adsorption mechanism of DBP and $CaCO_3$ exists, that is the binding of the abundant carbonyl groups of DBP with the Ca-O band of $CaCO_3$ from shells. This also could be proved by the drastic increase of DBP adsorption capacity from 400°C to 500 °C on the calcination temperature. The main component of shell calcinated below 400 °C is aragonite, while calcinated at 500 °C the main component turned to be calcite because the conversion temperature from aragonite to calcite lies in the range of 400-470 °C. Aragonite is a polymorph of calcite and has an orthorhombic symmetry, while calcite has the characteristic structure to trigonal symmetry with which could be more beneficial for the binding of C=O groups and Ca-O band.

3.4. Adsorption isotherms

According to section 2.2, the clam sea shell calcined at 500°C for 10mins had the best adsorption capacity, therefore its adsorption isotherm was investigated purposefully. Figure 7 was the relationship between equilibrium adsorption capacity (q_e) and equilibrium DBP concentration in solution (C_e). The trend of plots was exponential increasing with the equilibrium DBP concentration in solution increasing, which implied that the adsorption of DBP was not the ideal monolayer adsorption. There should be some interaction among the adsorbed DBP molecules and calcined shell.

The relationship between C_e and q_e was fitted by the Freundlich isotherm model, and the curve was shown in Figure 7. The correlation coefficient (R^2) was 0.9566, which implied that the model was appropriate for describing the adsorption isotherm of DBP onto the calcined clam seashell. K_F $(mg\cdot g^{-1})(L\cdot g^{-1})^{1/n}$, the constant related to sorption capacity, was 7.8697. n, the heterogeneity factor, was 1.6444.

3.5. Adsorption kinetics

Figure 8 showed the relationship between the adsorption capacity of DBP (q_t) and adsorption time (t) at 30°C. The data turned out that an adsorption time of 40mins was long enough for the adsorption process to reach equilibrium. The equilibrium adsorption capacity of DBP (q_e) was $1.2155 mg\cdot g^{-1}$. Two kinetics models were fitted to the data. The curves of the models were also shown in Figure 8.

The results showed that the pseudo-second-order-kinetics model was more appropriated for describing the adsorption process of DBP onto the calcined clam seashell. Its correlation coefficient (R^2) was 0.99372. k_2 $(g\cdot mg^{-1}\cdot min^{-1})$, the adsorption rate constant, was 0.7870. While the correlation coefficient of the pseudo-first-order-kinetics model was only 0.94122.

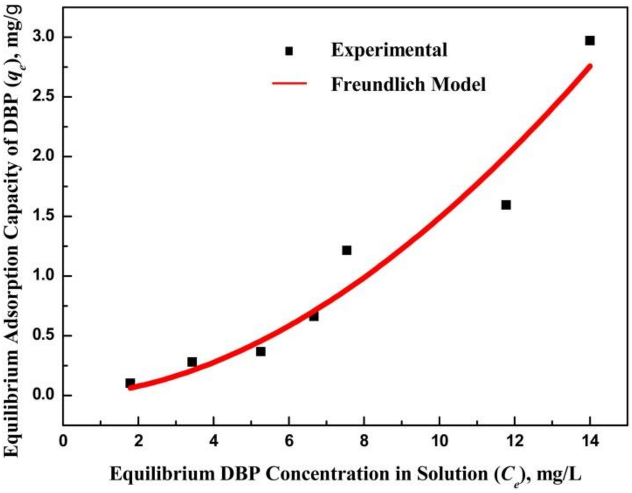

Figure 7. The relationship between equilibrium adsorption capacity (q_e) and equilibrium DBP concentration in solution (C_e)

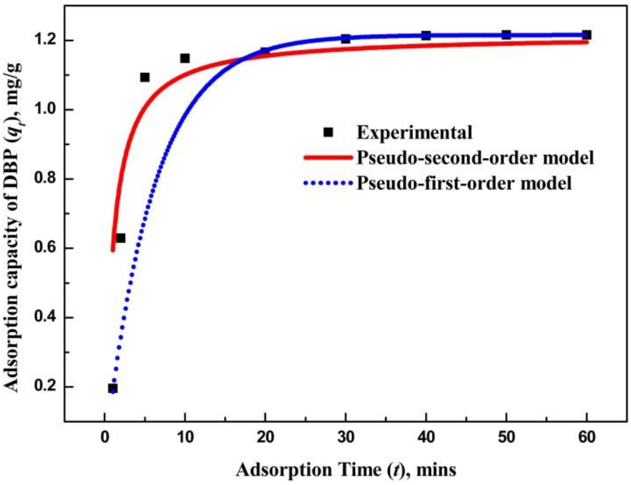

Figure 8. The relationship between adsorption capacity of DBP (q_t) and adsorption time (t) at 30°C

4. Conclusions

In this study, the calcined clam seashell powders were applied as adsorbents to adsorb DBP from an aqueous solution. The influence of calcination conditions on its adsorption capability to DBP was investigated. It was observed that the calcination conditions including temperature and time significantly affected the adsorption capabilities of clam seashells powders to the DBP. The calcination temperature has a strong influence on the adsorption capacity of the waste seashell and the maximum adsorption capacity as 1200 ug/g was achieved by the shell powder calcined at 500 °C. The calcination time influence the crystal unit cell sizes of $CaCO_3$ and the specific surface area of the clam seashells. The crystal unit cell Sizes show the tendency to increase at the first 10 mins then decrease to a stable size, while the specific surface area shows the opposite tendency with a decrease at the first 10 mins then increase. The DBP adsorption capacity changed as the same tendency as the crystal unit cell sizes of $CaCO_3$, which demonstrated the crystal unit cell sizes of $CaCO_3$ could influence greatly on the DBP adsorption property. The maximum adsorption capability and the largest unit cell size of $CaCO_3$ were simultaneously achieved at the calcination time of 10mins, which means the optimum calcination time could be 10mins. The kinetic studies revealed that the adsorption process best fit the pseudo-second-order kinetic model. The study on equilibrium sorption revealed that the Freundlich isotherm model gave the best fit to experimental data. The nature of adsorption of DBP on calcined sea shell powder was inferred as chemical adsorption.

Acknowledgment

This work is supported by the Hebei Science Technology Research Funds of China (20373604D).

Conflict of Interest

The authors declare no conflict of interest.

References

Akbari-Adergani B., Saghi M.H., Eslami A., Mohseni-Bandpei A. and Rabbani M. (2018), Removal of dibutyl phthalate from aqueous environments using a nanophotocatalytic Fe, Ag-ZnO/VIS-LED system: modeling and optimization. *Environmental Technology*, **39**(12), 1566–1576.

Ali I., Asim M. and Khan T. (2012), Low cost adsorbents for the removal of organic pollutants from wastewater. *Journal of Environmental Management*, **113**, 170–183.

Bhatnagar A., Kumara E. and Sillanp M. (2011), Fluoride removal from water by adsorption—A review. *Chemical Engineering Journal*, **171**, 811–840.

Bi J., Lu C., Wang Y. and Shao Y. (2002), Microstructure experiment and calcination characteristics of shells. *Journal of Chemical Industry and Engineering (China)*, **53**(11), 1128–1132.

Chowdhury S. and Saha P. (2010), Sea shell powder as a new adsorbent to remove Basic Green 4 (Malachite Green) from aqueous solutions: Equilibrium, kinetic and thermodynamic studies. *Chemical Engineering Journal*, **164**, 168–177.

Commission Staff Working Document on the Implementation of the Community Strategy for Endocrine Disrupters-A Range of Substances Suspected of Interfering with the Hormone System of Humans and Wildlife, 2007.

Doke K.M. and Khan E.M. (2013), Adsorption thermodynamics to clean up wastewater; critical review. *Reviews in Environmental Science and Bio/Technology*, (12), 25–44.

Du Y., Lian F. and Zhu L. (2011), Biosorption of divalent Pb, Cd and Zn on aragonite and calcite mollusk shells. *Environmental Pollution*, **159**, 1763–1768.

Lee Y. and Reeder R. (2006), The role of citrate and phthalate during Co(II) co-precipitation with calcite, *Geochimica et Cosmochimica Acta*, **70**, 2253–2263.

Li C. and Champagne P. (2009), Fixed-bed column study for the removal of cadmium (II) and nickel (II) ions from aqueous solutions using peat and mollusk shells. *Journal of Hazardous Materials*, **171**, 872–878.

Li H., Qin J., Zhang Y., Xu S., Du J. and Tang J. (2018), The efficiency and mechanism of dibutyl phthalate removal by copper-based metal organic frameworks coupled with persulfate. *RSC Advances*, **8**(69), 39352–39361.

Li L., Zhu W., Chen L., Zhang P. and Chen Z. (2005), Photocatalytic ozonation of dibutyl phthalate over TiO_2 film. *Journal of Photochemistry and Photobiology A: Chemistry*, **175**(2–3), 172–177.

Li R.L., Liang J., Gong Z.B., Zhang N.N. and Duan H.L. (2017), Occurrence, spatial distribution, historical trend and ecological risk of phthalate esters in the Jiulong River, *Southeast China Science of The Total Environment*, **580**, 388–397.

Lin A., Ding X., Xie Z. and Qian M. (2010), Microstructure of Patinopecten Yessoensis (Scallop) Shell and Correlations with Functions. *Journal of the Chinese Ceramic Society*, (3), 504–509.

National Standard of the People's Republic of China, 2016.

Obade V.P., Lal R. and Chen J. (2013), Remote Sensing of Soil and Water Quality in Agro ecosystems. *Water Air Soil Pollution*, **224**, 1658.

Peña-Rodríguez S., Bermúdez-Couso A., Nóvoa-Muñoz J.C., Arias-Estévez M., Fernández-Sanjurjo M.J., Álvarez-Rodríguez E. and Núñez-Delgado A. (2013), Mercury removal using ground and calcined mussel shell. *Journal of Environmental Sciences*, **25**(12), 2476–2486.

Qiu H., Lv L., Pan B., Zhang Q., Zhang W. and Zhang Q. (2009), Critical review in adsorption kinetic models. *Journal of Zhejiang University Science A*, **10**(5), 716–724.

Qureshi U.A., Solangi A.R., Memon S.Q., Taqvi S.I. and Memon N. (2012), Ionic liquid modified resin for the adsorptive removal of dibutyl phthalate: equilibrium, kinetic, and thermodynamic studies. *CLEAN–Soil, Air, Water*, **40**(6), 630–639.

Suresh S., Srivastava V.C. and Mishra I.M. (2012), Adsorption of catechol, resorcinol, hydroquinone, and their derivatives: a review. *International Journal of Energy and Environmental Engineering,* (**3)**, 32**.**

Teng H.H. and Dove P.M. (1997), Surface site-specific interactions of aspartate with calcite during dissolution: implications for biomineralization, *American Mineralogist*, **82**, 878–887.

Toxic Substances Control Act (TSCA) Work Plan, United States Environmental Protection Agency, 2014.

Wang X., Zhao K., Yang B., Chen T., Li D., Wu H., Wei J. and Wu X. (2016), Adsorption of dibutyl phthalate in aqueous solution by mesoporous calcium silicate grafted non-woven polypropylene. *Chemical Engineering Journal*, **306**, 452–459.

Xiong J., Qin Y., Islam E., Yue M. and Wang W. (2011), Phosphate removal from solution using powdered freshwater mussel shells. *Desalination*, **276**, 317–321.

Yan N. and Chen X. (2015), Sustainability: Don't waste seafood waste, *Nature*, **524**,155–157.

Yeom S.H. and Jung K.Y. (2009), Recycling wasted scallop shell as an adsorbent for the removal of phosphate. *Journal of Industrial and Engineering Chemistry*,**15**, 40–44.

Zhang W., Xu Z., Pan B., Hong C., Jiaa K., Jiang P., Zhang Q. and Pan B. (2008), Equilibrium and heat of adsorption of diethyl phthalate on heterogeneous adsorbents. *Journal of Colloid and Interface Science*, **325**, 41.

Zhang Z.H., Zhang C., Huang Z.H., Yi X.H., Zeng H., Zhang M.Z. and Huang M.Z. (2019), Residue levels and spatial distribution of phthalate acid esters in water and sediment from urban lakes of Guangzhou, China, *Journal of Environmental Science and Health, Part A*, **54**(2), 127–135.